Thin-filament pyrometry with a digital still camera

Jignesh D. Maun, Peter B. Sunderland, and David L. Urban

A novel thin-filament pyrometer is presented. It involves a consumer-grade color digital still camera with 6 megapixels and 12 bits per color plane. SiC fibers were used and scanning-electron microscopy found them to be uniform with diameters of 13.9 μm. Measurements were performed in a methane–air coflowing laminar jet diffusion flame with a luminosity length of 72 mm. Calibration of the pyrometer was accomplished with B-type thermocouples. The pyrometry measurements yielded gas temperatures in the range of 1400–2200 K with an estimated uncertainty of ±60 K, a relative temperature resolution of ±0.215 K, a spatial resolution of 42 μm, and a temporal resolution of 0.66 ms. Fiber aging for 10 min had no effect on the results. Soot deposition was less problematic for the pyrometer than for the thermocouple.

OCIS codes: 120.1740, 120.6780, 110.6820, 120.5630.

1. Introduction

Temperature is among the most commonly measured quantities in combustion research. Many methods are used to measure temperature owing to diverse flame configurations and hardware constraints. The temperature diagnostic considered here is thin-filament pyrometry (TFP). This diagnostic provides temperatures along lines with good temperature, spatial, and temporal resolution, fast thermal response times, and minimal invasiveness. This work seeks to develop an accurate TFP system using an inexpensive digital still camera.

TFP measures the radiative emissions of a thin fiber in a flame or other hot gas and determines temperatures from the radiative emissions. TFP was first used by Vilimpoc and Goss,[1] Vilimpoc *et al.*,[2] and Goss *et al.*[3] following the development by Ferguson and Keck[4] of a hot-wire pyrometer. The initial TFP systems[1–3] used 15 μm β-SiC fibers, InGaAs single-element infrared detectors (sensitive to wavelengths of 900–1600 nm), rotating mirrors, and calibration using a steady flame of known temperature. Other researchers have performed TFP using single-element detectors with either rotating mirrors or traversable flames.[5–8]

The use of cameras for TFP was introduced by Bédat *et al.*[9] This was advanced by Pitts[10] and Pitts *et al.*,[11] who performed TFP using a cooled 16-bit charge-coupled device (CCD) video camera sensitive to visible and near-infrared light and an imaging area of 540 × 61 pixels. Other studies have used cooled CCD cameras for TFP, such as a 1100 × 330 pixel 16-bit camera,[12] but these cameras were costly and had limited pixel counts. A consumer-grade digital still camera with 1712 × 1368 pixels reduced the cost but was limited to 8 bits and was used only for qualitative TFP.[13] Another 8-bit CCD camera, of unspecified pixel dimensions, was used by Bundy *et al.*[14] Using cameras for TFP simplifies alignment and allows simultaneous scans along one or more fibers. It also facilitates corrections for luminosity from soot and hot gases. However no past TFP study has used a camera with a high bit depth, a high pixel count, and a low cost.

A Nikon D70 digital still camera, similar to the camera used here, was used for soot pyrometry by Connelly *et al.*[15] That study found the camera to be linear and repeatable and to be adequate for quantitative soot pyrometry.

Given the extensive past interest in TFP and the advent of inexpensive digital still cameras, the objectives of this work are to

(1) demonstrate the use of a digital still camera for TFP,
(2) evaluate the suitability of TFP in flame regions with light soot loading, and
(3) examine representative SiC fibers with a scanning electron microscope.

J. D. Maun and P. B. Sunderland (pbs@umd.edu) are with the Department of Fire Protection Engineering, University of Maryland, College Park, Maryland 20742. D. L. Urban is with the Combusting and Reacting Systems Branch, NASA Glenn Research Center, Cleveland, Ohio 44135.

Received 17 July 2006; revised 27 September 2006; accepted 28 September 2006; posted 29 September 2006 (Doc. ID 73068); published 17 January 2007.

0003-6935/07/040483-06$15.00/0

The present TFP system is calibrated using thermocouple measurements in a methane–air coflowing laminar gas jet diffusion flame.

2. Experimental

The test flame was a coflowing methane–air laminar jet diffusion flame with a luminosity length of 72 mm (prior to fiber insertion) burning at atmospheric pressure. Methane (99.99% purity) flowed upward through a 14 mm round port at 4.3 mg/s. Air flowed upward through a ceramic honeycomb and out of a 100 mm round coflow port at 1.7 g/s. The fuel port extended 2 mm beyond the air port. Flow rates were measured and monitored with calibrated rotameters. The flame was sufficiently stable that no chimney or screen was needed. Details of the experimental configuration are given by Maun.[16]

The SiC fibers were 13.9 μm in diameter and were composed of Si, C, and O with mass fractions of 0.57, 0.32, and 0.12. These fibers were manufactured by Nippon Carbon Company (Tokyo) and distributed by Dow Corning (Midland, Michigan) under the name Nicalon. (Certain commercial equipment and materials are identified here to specify the experimental procedure adequately. This does not imply endorsement or recommendation by NASA.) The fibers contain ultrafine β-SiC crystals and an amorphous mixture of silicon, carbon, and oxygen. These fibers are used most commonly in fabrics and composite materials. They were coated by the manufacturer with polyvinyl alcohol (PVA) to improve handling characteristics for fabric manufacture. The fibers were provided on a spool as bundled yarn with a diameter of ~1 mm. The yarn was readily unraveled to provide the single-strand fibers used here.

Fibers 120 mm long were held taut in a frame and were positioned horizontally in the methane–air flame. The frame was attached to a translation stage to facilitate alignment and to allow the fibers to be heated to glowing in hot lean flame regions prior to each test. This heating ensured the removal of any residual PVA and soot.

Scanning electron microscopy (SEM) was performed with an ElectroScan E3-ORI-103 microscope. SEM yielded surface images of representative SiC fibers and was used to measure fiber diameters.

The flame and fibers were imaged with a Nikon D100 single-lens reflex color digital still camera. A Nikon 60 mm 2.8 focal length (f) autofocus (AF) lens was used at 3.3f. The camera contains a rectangular CCD of 23.7 × 15.6 mm with 3008 × 2000 pixels (6 megapixels) and an infrared blocking filter. The CCD was 445 mm from the flame axis and the optical axis was 50 mm above the burner port. The spatial resolution in the object plane was 42 μm/pixel. The International Organization for Standardization (ISO) film speed was set at 200 and the shutter time for TFP measurements was 0.66 ms. All automatic camera settings were disabled, namely, those associated with focus, aperture, shutter speed, ISO, exposure compensation, tone, hue, white balance, image sharpening, and noise reduction. The D100 is a consumer-grade camera. It is no longer produced, but has been replaced with the D70, whose specifications are nearly identical.

Each pixel of the D100 is sensitive to red, green, or blue (RGB). The camera's interpolation yields 12 bit RGB intensities at each pixel at a bit depth of 12 (i.e., a range of 0–4095). Initial images of glowing fibers revealed red and green intensities were far greater than blue intensities. Two changes were made to better equalize these: a 3 mm thick 50 mm × 50 mm Schott blue-green (BG) 26 blue filter[15] was placed in front of the lens and a white balance of incandescent with a color temperature of 2700 K was selected. Camera exposures were chosen such that the fiber images were bright but did not saturate at any pixel in any color plane.

Images were recorded in Adobe RGB color space and saved in uncompressed 12 bit Nikon electronic image format. They were then converted to color tagged image file (tif) format using Nikon Capture Editor software (V3.5). Note that newer versions of this software caused a fidelity loss during this conversion. The tif images were analyzed using the SPOTLIGHT 16 software (V2004.8.27) of Klimek *et al.*[17]

Flame luminosity, especially from soot, can interfere with TFP. Flame luminosity was negligible at a height of 11 mm above the fuel port. However, at a height of 21 mm there was sufficient soot luminosity that compensation was warranted. For TFP at this height separate images were recorded with and without fibers present. An image without fibers was then subtracted from each image with fibers using SPOTLIGHT 16 software. After subtraction any negative RGB intensities were set to zero.

SPOTLIGHT 16 software was used to extract from the images the RGB intensities and pixel locations along the fibers. RGB intensities were averaged for five pixels perpendicular to the fibers, corresponding to the approximate full width at half-maximum (FWHM) widths of the brightest imaged regions of the glowing fibers. Gray scales were calculated as the average of RGB intensities.

The TFP system was calibrated with thermocouple measurements in the methane–air diffusion flame. Thermocouple temperatures (T_{TC}) were measured and were corrected for radiative losses to obtain gas temperatures (thermocouple-derived T_{gas}) and fiber temperatures (thermocouple-derived T_{fiber}). Measured fiber intensities were then calibrated with these fiber temperatures. Finally, this calibration was used to convert the fiber intensities to fiber temperatures (TFP-derived T_{fiber}), to which radiative corrections were made to obtain gas temperatures (TFP-derived T_{gas}). Details are provided below.

The thermocouple was an uncoated B-type thermocouple (Pt − 30% Rh versus Pt − 6% Rh) with a wire diameter of 51 μm and a butt-welded junction of the same diameter.[18] The thermocouple supports were 20 mm apart to minimize disturbances. The thermocouple was positioned horizontally, with the flame axis closer to the junction than to any other part of the probe. Raw thermocouple temperatures were av-

eraged over 60 s except at the flame sheet (the peak temperature zone), where peak instantaneous temperatures were recorded and then averaged. Thermocouple measurements were not recorded where soot deposited, a condition that was identified by temperatures that decreased with time, because steady measurements were impossible and surface emissivity was unknown.

A detailed analysis of convection, radiation, and conduction for steady-state cylindrical probes (e.g., thermocouples or fibers) is provided by Maun.[16] This results in the following heat balance:

$$h(T_{gas} - T_{cyl}) = \sigma\varepsilon(T_{cyl}^4 - T_\infty^4) - (k_{cyl}d_{cyl}/4)\mathrm{d}^2T_{cyl}/\mathrm{d}x^2, \quad (1)$$

where h is the heat transfer coefficient, *cyl* denotes cylinder, σ is the Stefan–Boltzmann constant, ε is graybody emissivity, T_∞ is ambient temperature, k is thermal conductivity, d is diameter, and x is the distance along the cylinder. Emissivities of the thermocouple and the fibers were taken to be 0.2 (Ref. 19) and 0.88,[3,5,6,10] respectively. Thermal conductivities of the thermocouple and the fibers were taken to be 69.87 and 2.2 W/m K, respectively. Conduction was found to be negligible for the thermocouple, owing to its alignment, and for the fibers, owing to their small k and d.[1,3,16]

The convective heating rate was obtained from Nakai and Okazaki[20] for Pe < 0.2:

$$\mathrm{Nu} = [0.8237 - 0.5\ln(\mathrm{Pe})]^{-1}, \quad (2)$$

where Nusselt and Peclet numbers are

$$\mathrm{Nu} = hd_{cyl}/k_{gas}, \qquad \mathrm{Pe} = ud_{cyl}/\alpha_{gas}, \quad (3)$$

u is the velocity, and α is the thermal diffusivity. Gas properties in Eq. (3) were assumed to be those of nitrogen at the average of the cylinder and gas temperatures. Velocity was estimated at 1 m/s based on velocity measurements near the flame sheet in similar flames.[21,22]

Raw thermocouple temperatures have an estimated uncertainty of ± 20 K. The thermocouple-derived T_{gas} measurements have estimated uncertainties that increase with T_{gas}, are up to ± 40 K, and arise from uncertainties in T_{TC} and the radiation corrections. Uncertainties in the thermocouple-derived fiber temperatures are estimated at up to ± 30 K. This is lower than uncertainties in T_{gas} because radiation corrections [Eq. (1)] were first added to the T_{TC} measurements to obtain T_{gas}, and then similar radiation corrections were subtracted from T_{gas} to obtain the thermocouple-derived fiber temperatures.

3. Results

Accurate TFP requires fibers with uniform diameter and surface composition. Representative SiC fibers were examined by SEM to address this. Figure 1(a) shows a SEM image of a typical new SiC fiber. This fiber is a smooth cylinder with an irregular coating. The coating, believed to be the PVA applied by the manufacturer, was found to be easily removed by treating fibers (heating them to glowing) in fuel-lean regions of the methane–air flame. A SEM image of a typical SiC fiber following such treatment is shown in Fig. 1(b). Treated fibers had smooth and uniform surfaces and thus fibers were treated prior to each TFP measurement. Mean diameters of treated fibers were measured in the SEM and were found to be 13.9 μm (in agreement with the manufacturer's value of 14 μm) with a standard deviation of 0.19 μm.

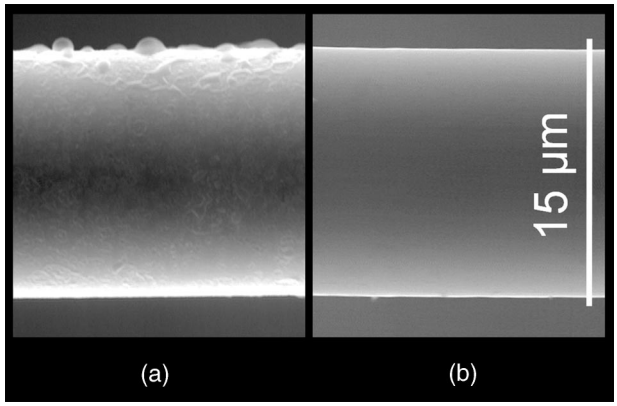

Fig. 1. (a) Gray scale SEM image of a typical new SiC fiber, and (b) gray scale SEM image of a typical treated SiC fiber.

Although the present fibers contain 12% (by mass) oxygen, they are not fully oxidized and are subject to further oxidation (aging) when placed in hot lean flame regions. Several unaged fibers were aged by placing them in the test flame for 10 min. These aged fibers appeared the same in SEM as unaged treated fibers. TFP measurements performed with aged and unaged fibers revealed no statistically significant differences. Following 60 min of aging, however, the fibers were observed to change from black to gray.

A color image of the test flame with a dark background is shown in Fig. 2. This image is identical to the images used for TFP except that here the blue Schott filter was removed, a white balance of direct sunlight was used, and a longer exposure was selected (resulting in saturation in some regions). The test flame is attached to the burner, and its luminosity length is 72 mm prior to fiber insertion and 69 mm following insertion. Yellow emissions from soot first appear near the flame sheet at a height of ~9 mm. The flame was nearly steady but wavered slightly.

Horizontal fibers at 11 and 21 mm heights are seen glowing in the image. These heights were chosen because they allow TFP to be examined at 11 mm with almost no soot and at 21 mm where moderate soot is present. The fibers were moved into position approximately 2 s before the image was recorded to minimize soot deposition at 21 mm height near the flame. Despite flame and soot luminosity, the fibers were brighter than their surroundings. The brightest regions of the imaged glowing fibers had mean widths

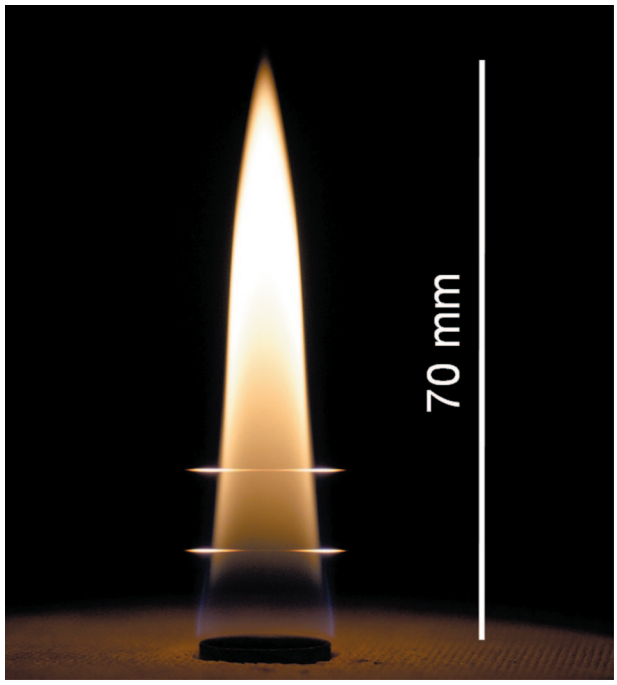

Fig. 2. Color image of the coflowing methane–air laminar jet diffusion flame with horizontal fibers at 11 and 21 mm heights. Exposure settings were 3.3*f*, ISO 200, and 8 ms.

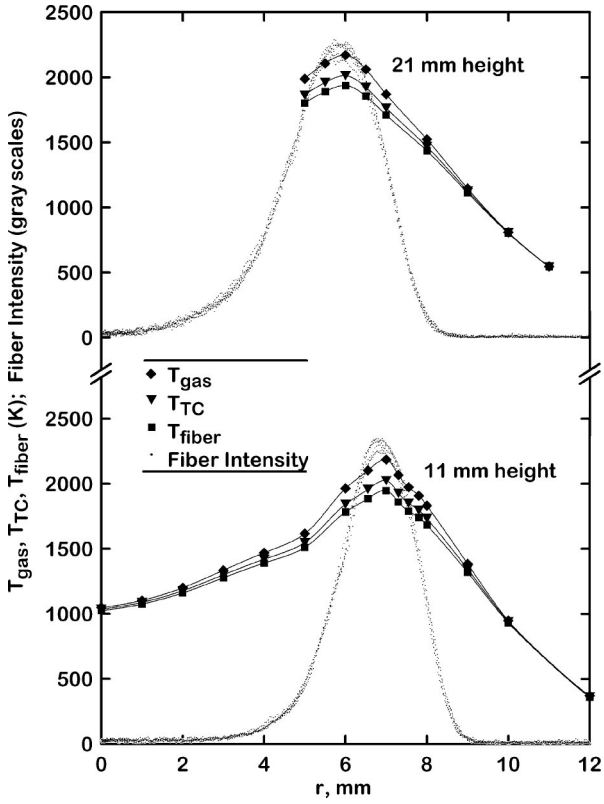

Fig. 3. Thermocouple-derived temperature measurements (T_{gas}, T_{TC}, T_{fiber}) and fiber gray-scale intensities at 11 and 21 mm heights. At each height 1710 fiber intensity data points are shown.

of 4.5 pixels FWHM, corresponding to a width in the object plane of 190 μm. Regions of the fibers that were 20% as bright had mean widths of 3.2 pixels FWHM. This increase in imaged fiber width upon heating has been reported before[13] and also is evident to the unaided eye. Its cause is unknown by the authors.

Figure 3 shows the three types of thermocouple-derived temperatures at 11 and 21 mm heights. At 11 mm and at most 21 mm locations no soot deposited on the thermocouple. However, at 21 mm within 5 mm of the flame axis soot deposition was detected, and thus thermocouple measurements are not reported. Triangles indicate the raw thermocouple measurements. Also shown are the thermocouple-derived gas temperatures (T_{gas}), which corrected for radiative losses. The highest T_{gas} observed, 2186 K, is reasonable considering the adiabatic flame temperature of methane–air of 2223 K.[23] Figure 3 also includes the thermocouple-derived estimates of T_{fiber}, which are up to 238 K cooler than the gas. Radiative temperature corrections increase approximately with the product of emissivity times cylinder diameter, which is higher for the fibers than for the thermocouple.

Figure 3 also includes measured fiber gray-scale intensities. These come from four images: three with fibers and one without. Concerning the three images with fibers, one involved a pair of aged fibers, the other two involved unaged fibers, and all the fibers were replaced between images to test for fiber independence. The fiber intensities at 21 mm height (but not at 11 mm) were obtained after image subtraction. Each fiber crossed the flame sheet twice and thus yielded two intensity profiles in Fig. 3. The data spacing along each profile is 42 μm. Each profile was shifted slightly to account for small variations in flame location. The peak fiber intensities are ~2300 gray scales. Longer exposures would have resulted in saturation (intensities of 4095) in the red and green color planes. Note that filament intensities are reported at a 21 mm height even near the flame axis where soot deposition impeded thermocouple measurements. Soot deposition was less problematic for TFP because it had less effect on probe emissivity, and the measurements were completed more quickly.

The thermocouple-derived T_{fiber} versus radius data of Fig. 3 were fitted with polynomials of order 3–6 (two polynomials at 11 mm height and one at 21 mm). These polynomials were used to associate most of the fiber intensity measurements of Fig. 3 with thermocouple-derived fiber temperatures. At a 21 mm height, this was performed only where thermocouple data were available, i.e., for radii in the range of 5–11 mm. This yielded a correlation between thermocouple-derived fiber temperature and fiber intensity, shown in Fig. 4, where both 11 and 21 mm heights are included. Figure 4 is the TFP calibration plot. The data are shown fit with a line for 1000–1350 K and a fifth-order polynomial for temperatures above 1350 K. The correlation is good for fiber temperatures above 1350 K, where typical scatter about the fit is ±20 K. For fiber temperatures above 1500 K

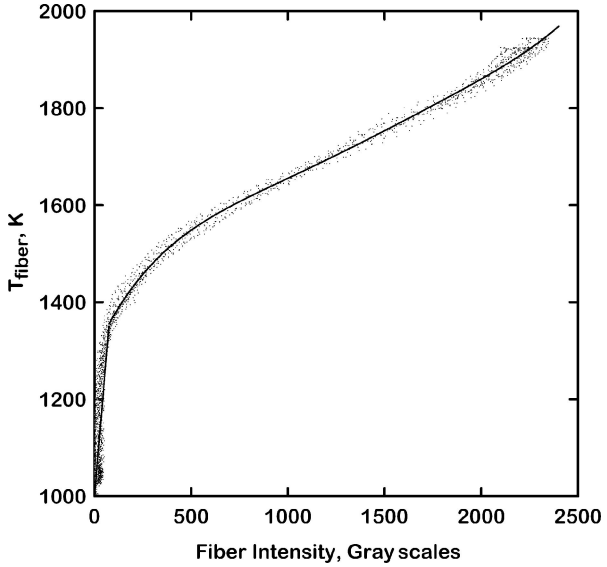

Fig. 4. Calibration plot of the TFP diagnostic. Thermocouple-derived fiber temperatures are plotted versus fiber intensities and 2070 data points are shown.

the data are reasonably well-represented by a linear relationship (not shown) between temperature and fiber intensity with a slope of 0.215 K/gray scale. This indicates that the relative precision of these TFP measurements is 0.215 K.

A comparison of gas temperatures measured by TFP and by thermocouple is shown in Fig. 5. Here the fiber intensities of Fig. 3 were converted to fiber temperatures using the above calibration. Radiation corrections were then applied to obtain TFP-derived gas temperatures. These TFP measurements were calibrated by the very thermocouple measurements to which they are compared in Fig. 5. Nevertheless this figure indicates the amount of scatter and the range of temperatures obtainable with this TFP system when six different fibers are used in diverse regions of this methane–air flame. If this calibrated TFP system were applied to any similar flame, comparable agreement with thermocouple data would be expected.

Figure 5 shows that the TFP diagnostic agrees well with thermocouple measurements for gas temperatures in the range of 1400–2200 K. In consideration of this plot and estimated thermocouple uncertainties, it is estimated that the uncertainty in the TFP-derived gas temperatures is ± 60 K for gas temperatures above 1400 K. TFP scatter increases below this temperature owing to limited camera sensitivity, but additional images at longer exposures show that gas temperatures as low as 800 K can be measured with the present TFP system. This lower temperature limit could probably be reduced by removing the infrared blocking filter that was installed in the camera during its manufacture.

Data in Fig. 5 at 21 mm height illustrate how regions of light soot loading (at radii below 5 mm) allow temperature measurements by TFP where thermocouple measurements are problematic. However, even TFP can be impeded at higher soot concentrations owing to increased soot deposition rates, increased background luminosity, and fiber luminosity extinction by optically thick surroundings.

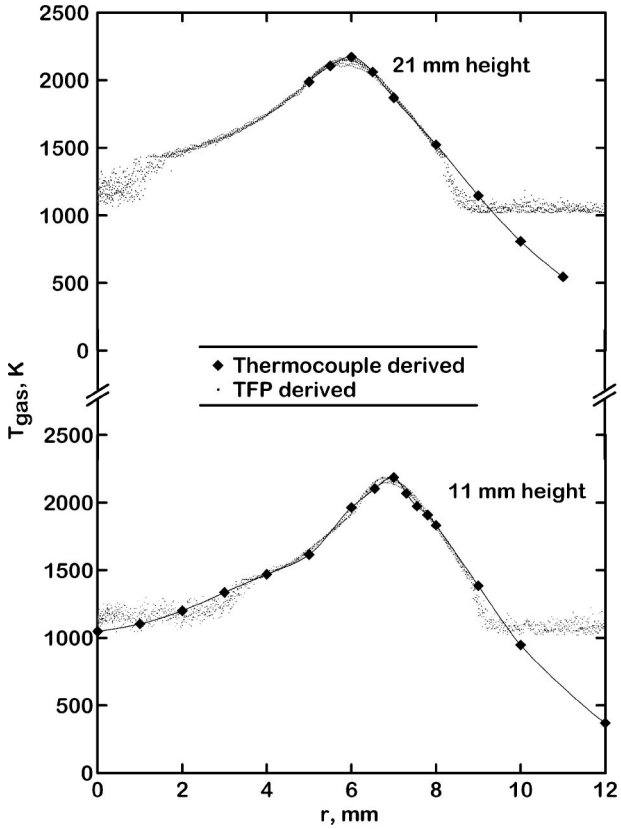

Fig. 5. TFP-derived and thermocouple-derived gas temperatures versus radius at 11 and 21 mm heights. These thermocouple measurements are reproduced from Fig. 3.

TFP has been demonstrated quantitatively here using a consumer-grade digital camera. This should make this diagnostic affordable to an increased number of users. In addition, the durability and self-contained operability of this camera should facilitate the use of TFP in drop towers and other microgravity or elevated-gravity facilities.

4. Conclusions

Thin-filament pyrometry was conducted in a methane–air laminar diffusion flame using a digital still camera. Thermocouple measurements were performed to calibrate the TFP system. The principal findings are:

(1) TFP has been demonstrated with an inexpensive digital color still camera. This 12-bit camera has the highest pixel resolution (3008×2000) of any camera used to date for TFP. The camera's low cost and high performance make it well suited for TFP. Its durability and self-contained operability allow its use in microgravity drop towers.

(2) The TFP system yielded gas temperatures in the range of 1400–2200 K with an estimated uncer-

tainty of ±60 K, a relative temperature resolution of ±0.215 K, a spatial resolution of 42 μm, and a temporal resolution of 0.66 ms.

(3) TFP was less susceptible to soot interference than was the thermocouple technique in this flame. Soot deposition on the thermocouple resulted in unsteadiness and an unknown emissivity.

(4) The present SiC fibers were found by SEM to have a mean diameter of 13.9 μm with a standard deviation of 0.19 μm. Six different fibers yielded identical intensities in the present flames within experimental uncertainties. Aging the fibers in a hot flame zone for 10 min had no effect on the appearance of the fibers in the scanning electron microscope or on the TFP measurements.

This work was supported by the NASA Glenn Research Center under grant NNC05GA59G. Assistance with the measurements was provided by T. Zhang and A. M. Levine. The authors are grateful for discussions with R. L. Axelbaum, P. S. Greenberg, A. W. Marshall, and J. G. Quintiere.

References

1. V. Vilimpoc and L. P. Goss, "SiC-based thin-filament pyrometry: theory and thermal properties," Proc. Combust. Inst. **22,** 1907–1914 (1988).
2. V. Vilimpoc, L. P. Goss, and B. Sarka, "Spatial temperature-profile measurements by the thin-filament-pyrometry technique," Opt. Lett. **13,** 93–95 (1988).
3. L. P. Goss, V. Vilimpoc, B. Sarka, and W. F. Lynn, "Thin-filament pyrometry: a novel thermometric technique for combusting flows," J. Eng. Gas Turbines Power **111,** 46–52 (1989).
4. C. R. Ferguson and J. C. Keck, "Hot-wire pyrometry," J. Appl. Phys. **49,** 3031–3032 (1978).
5. L. G. Blevins, M. W. Renfro, K. H. Lyle, N. M. Laurendeau, and J. P. Gore, "Experimental study of temperature and CH radical location in partially premixed CH_4/air coflow flames," Combust. Flame **118,** 684–696 (1999).
6. R. V. Ravikrishna and N. M. Laurendeau, "Laser-induced fluorescence measurements and modeling of nitric oxide in methane-air and ethane-air counter-flow diffusion flames," Combust. Flame **122,** 474–482 (2000).
7. J. Ji, Y. R. Sivathanu, and J. P. Gore, "Thin filament pyrometry for flame measurements," Proc. Combust. Inst. **28,** 391–398 (2000).
8. S. D. Marcum and B. N. Ganguly, "Electric-field-induced flame speed modification," Combust. Flame **143,** 27–36 (2005).
9. B. Bédat, A. Giovannini, and S. Pauzin, "Thin filament infrared pyrometry: instantaneous temperature profile measurements in a weakly turbulent hydrocarbon premixed flame," Exp. Fluids **17,** 397–404 (1994).
10. W. M. Pitts, "Thin-filament pyrometry in flickering laminar diffusion flames," Proc. Combust. Inst. **26,** 1171–1179 (1996).
11. W. M. Pitts, K. C. Smyth, and D. A. Everest, "Effects of finite time response and soot deposition on thin filament pyrometry measurements in time-varying diffusion flames," Proc. Combust. Inst. **27,** 563–569 (1998).
12. P. Struk, D. Dietrich, R. Valentine, and I. Feier, "Comparisons of gas-phase temperature measurements in a flame using thin-filament pyrometry and thermocouples," in *Proceedings of the American Institute of Aeronautics and Astronautics 41st Meeting* (AIAA, 2003).
13. S. H. Shim and H. D. Shin, "Application of thin SiC filaments to the study of coflowing, propane/air diffusion flames: a review of soot inception," Combust. Sci. Tech. **175,** 207–223 (2003).
14. M. Bundy, A. Hamins, and K. Y. Lee, "Suppression limits of low strain rate non-premixed methane flames," Combust. Flame **133,** 299–310 (2003).
15. B. C. Connelly, S. A. Kaiser, M. D. Smooke, and M. B. Long, "Two-dimensional soot pyrometry with a color digital camera," in *Proceedings of the Fourth Joint Meeting of the U.S. Sections of the Combustion Institute* (Combustion Institute, 2005).
16. J. D. Maun, "Thin-filament pyrometry with a digital still camera," M.S. thesis (University of Maryland, 2006).
17. R. B. Klimek, T. W. Wright, and R. S. Sielken, *Color Image Processing and Object Tracking System,* NASA Technical Memorandum 107144 (NASA Lewis Research Center, 1996).
18. P. B. Sunderland, R. L. Axelbaum, D. L. Urban, B. H. Chao, and S. Liu, "Effects of structure and hydrodynamics of the sooting behavior of spherical microgravity diffusion flames," Combust. Flame **132,** 25–33 (2003).
19. D. Bradley and A. G. Entwistle, "Determination of the emissivity, for total radiation, of small diameter platinum-10% rhodium wires in the temperature range 600–1450 °C," B. J. Appl. Phys. **12,** 708–711 (1961).
20. S. Nakai and T. Okazaki, "Heat transfer from a horizontal circular wire at small Reynolds and Grashof numbers—I pure convection," Int. J. Heat Mass Transfer **18,** 387–396 (1975).
21. R. J. Santoro, T. T. Yeh, J. J. Horvath, and H. G. Semerjian, "The transport and growth of soot particles in laminar diffusion flames," Combust. Sci. Technol. **53,** 89–115 (1987).
22. P. B. Sunderland and G. M. Faeth, "Soot formation in hydrocarbon/air laminar jet diffusion flames," Combust. Flame **105,** 132–146 (1996).
23. B. Lewis and G. von Elbe, *Combustion, Flames and Explosions of Gases* (Academic, 1987), p. 720.